LA-9597-MS

Los Alamos National Laboratory is operated by the University of California for the United States Department of Energy under contract W-7405-ENG-36.

SHALO—A Simple Theoretical Description of Drainage Flow

Los Alamos Los Alamos National Laboratory
Los Alamos, New Mexico 87545

LA-9597-MS

UC-66a
Issued: December 1982

SHALO—A Simple Theoretical Description of Drainage Flow

Burton E. Freeman*
Cecil G. Davis
Susan S. Bunker

*Consultant at Los Alamos. Physical Dynamics, Inc., P.O. Box 556, La Jolla, CA 92038.

Los Alamos National Laboratory
Los Alamos, New Mexico 87545

SHALO--A SIMPLE THEORETICAL DESCRIPTION OF DRAINAGE FLOW

by

Burton E. Freeman, Cecil G. Davis, and Susan S. Bunker

ABSTRACT

A model for drainage flow has been developed using shallow fluid theory and considerations of entrainment of overlying air and surface drag. Using explicit differencing techniques, we have produced a code and applied it to the nocturnal drainage flows in the complex valleys of the geysers geothermal area of northern California.

I. INTRODUCTION

The drainage flow problem has several physically simple, yet computationally difficult, effects. The process, by definition, is dominated by terrain. Fluid displacements are large compared to terrain features; entrainment of overlying air is significant; pressure forces (through buoyancy terms) dominate the motion; and thermodynamic processes are responsible for these forces. Computationally, a mixed system consisting of Lagrangian-in-vertical and Eulerian-in-horizontal coordinates is advantageous. The validity of the hydrostatic approximation simplifies the problem.

The shallow fluid approximation has been used extensively for oceanic applications (estuaries, coastal upwelling, and gravity surges) and for meteorology (mountain waves, frontal behavior, and boundary-layer flow) but has not been applied to the drainage flow problem explicitly. The boundary layer applications[1,2] have been limited because they neglect vertical structure in the entire boundary layer and omit several relevant physical processes. Recently, the physical effects have been given attention[3] and the drainage flow application of this approximation is particularly favorable. In

addition, the mathematical problem of frontal motion may be alleviated by the inclusion of entrainment. Consequently, the formulation described below, when applied to drainage flow, may have several advantages not evident in previous meteorological applications of the shallow fluid approximation.

A generalization of the shallow fluid approximation developed for application to drainage flows is reported below. A single fluid layer having variable depth and density as a function of position and time describes the average behavior of the flow yet retains a substantial degree of ease of formulation and computational economy. In exchange, all details of the layer substructure are lost, such as profiles of velocity, temperature, etc. The single-layer shallow fluid formulation has the following characteristics:

(1) layer thickness varies with position and time over complex terrain.

(2) additional variables associated with the layer are the velocity, potential temperature, and pollutant concentration.

(3) entrainment of overlying air and surface drag accelerate the flow.

(4) density changes are driven by a rudimentary energy budget calculation in which terrestrial radiation cooling is the most important term.

(5) an explicit difference formulation is feasible because the flow speed and the gravity wave phase speed are small.

II. DERIVATION OF EQUATIONS

The model is based on Fig. 1, which shows two layers.

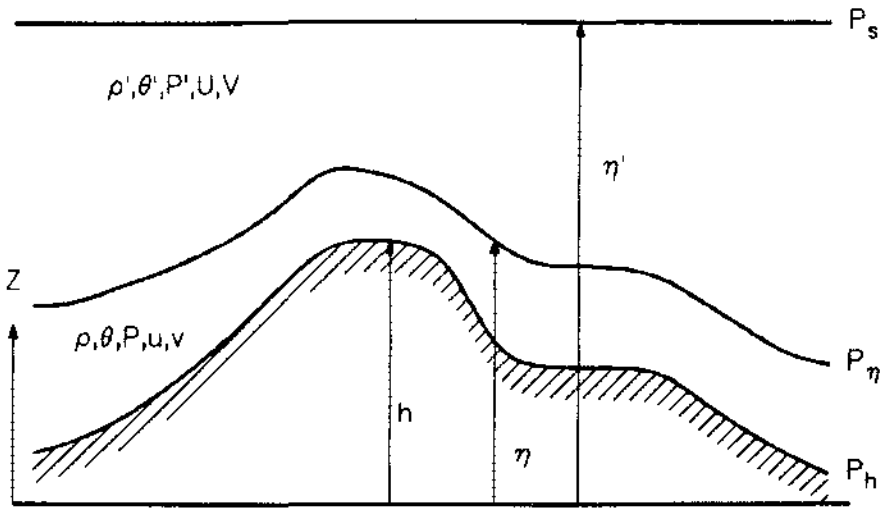

Fig. 1. Description of shallow fluid model.

The layer adjoining the terrain with thickness $\eta - h$ is the drainage layer. The "primed" layer with thickness $\eta' - \eta$ is used for calculating the pressure forces; we assume $\nabla\eta' = 0$ and $\theta' = \text{constant}$, where

$$\nabla = \hat{i}\,\frac{\partial}{\partial x} + \hat{j}\,\frac{\partial}{\partial y}$$

is the horizontal gradient operator. Within the drainage layer, the velocity components u and v, the density ρ, the temperature θ, and the pressure P are also functions of (x, y, t). We assume that the pressure P_S on the surface η' serves as the large-scale force giving rise to the geostrophic wind. Consequently, we allow $\nabla P_s \neq 0$.

To calculate the pressure forces on the $\eta - h$ layer, the hydrostatic relation is used:

$$\frac{dP}{dZ} = -g\rho \quad ,$$

where Z is the altitude and g is the acceleration from gravity. To account for the density gradient in the layers caused by compressibility, the equation

of state, $P = \rho RT$, and the adiabatic relation, $T = \theta(P/P_o)^s$ (where $s = R/C_p = 0.286$), are used to reformulate the hydrostatic relation,

$$Z_2 - Z_1 = \frac{R}{g\, P_o^s} \int_{P_2}^{P_1} \frac{\theta dP}{P^{1-s}} \quad . \tag{1}$$

Assuming for the pressure calculation that θ and θ' are independent of Z (or P) and solving for P,

$$P(Z) = P_o \left[\left(\frac{P_s}{P_o} \right)^s + \frac{sg}{R} \left(\frac{\eta - Z}{\theta} + \frac{\eta' - \eta}{\theta'} \right) \right]^{1/s} , \quad h \leq Z \leq \eta \quad . \tag{2}$$

The force F on a unit area of the layer is

$$F = P(Z = \eta)\ \nabla\eta - P(Z = h)\ \nabla h - \nabla \int_h^\eta P dZ \quad . \tag{3}$$

After some algebraic reduction, the following expression for the force is obtained

$$F = -\left[F_2^{1/s} - F_1^{1/s} \right] \left[P_o \left(1 - \frac{\theta}{\theta'} \right) \nabla\eta + \frac{R\theta}{g} \left(\frac{P_o}{P_s} \right)^{1-s} \nabla P_s \right]$$
$$+ \frac{P_o R}{(s+1)g} \nabla\theta \left\{ F_1^{1+\frac{1}{s}} - \left[F_1 - \frac{\eta - h}{\theta} \frac{g}{R} \right] F_2^{1/s} \right\} \quad , \tag{4}$$

where

$$F_1 = \left(\frac{P_s}{P_o} \right)^s + \frac{sg}{R} \frac{\eta' - \eta}{\theta'} \quad \text{and}$$

$$F_2 = F_1 + \frac{sg}{R} \frac{\eta - h}{\theta} \quad .$$

For small layer thicknesses, the coefficient of the first terms is proportional to the drainage layer thickness $\eta - h$, whereas the coefficient of the temperature gradient term is proportional to the square of the drainage layer thickness. The terms in Eq. (4) are interpreted as follows:

(1) the term proportional to $\nabla\eta$ is the buoyancy force containing a factor $1 - \theta/\theta'$ for reduced gravity.

(2) the term proportional to ∇P_s is the large-scale pressure (or geostrophic) force.

(3) the $\nabla\theta$ term is due to horizontal density gradients arising from differential heating or entrainment.

The terms have been compared and checked against the simpler case of constant density layers. There is no term containing ∇h because it is not the terrain that causes the acceleration (a flat-surfaced lake is in an equilibrium configuration) but the sloping surface and horizontal density gradients.

Schematically, the other terms entering the equations of motion are

(1) the terrain drag force $F_D = -\bar{\rho} C_D |u| \underline{u}$, where C_D is a drag coefficient that may depend on surface roughness, flow speed, and temperature difference between ground and air, and $\underline{u}$ is the layer velocity;

(2) the Coriolis force $F_C = -\bar{\rho}(\eta - h)\ \underline{\Omega} \times \underline{u}$, where $\underline{\Omega}$ is twice the angular rotation vector of the Earth;

(3) the momentum entrainment $\dot{m}\underline{U}$, where $\underline{U}$ is the "primed" layer velocity and the mass entrainment rate depends on relative velocity and density of the two layers and on the lower layer thickness; and

(4) lateral diffusion $F_\Delta = O(u_i)$, where the operator

$O = \rho(\eta - h)\, D \dfrac{\partial^2}{\partial x_j^2}$ and D is the lateral diffusion coefficient.

Using the above quantities, the governing equations for the drainage layer can now be written. Each equation pertains to a property (mass, momentum, etc.) of the drainage layer as a whole.

Mass

$$\frac{\partial \bar{\rho}(\eta - h)}{\partial t} + \frac{\partial}{\partial x_i} \overline{\rho u_i}(\eta - h) = \dot{m} \quad , \tag{5}$$

where the overbar indicates an average of the quantity over the height interval $\eta - h$. This equation determines the rate of change of mass in each x, y cell caused by flow to adjacent cells and entrainment. The averaging is discussed below.

Momentum

$$\frac{\partial \overline{\rho u_i}(\eta - h)}{\partial t} + \frac{\partial}{\partial x_j} \overline{\rho u_i u_j}(\eta - h) = \dot{m}\, U_i + F + F_D + F_{C\,i} + O(u_i) \quad . \qquad (6)$$

This equation determines the velocity components when the mass is known. The effects accounted for are entrainment, pressure forces, terrain drag, Coriolis force, and lateral diffusion, as well as advection.

Potential Temperature

$$\frac{\partial \overline{\rho\theta}(\eta - h)}{\partial t} + \frac{\partial}{\partial x_i} \overline{\rho u_i \theta}(\eta - h) = \dot{m}\theta' + \frac{\dot{H}}{C_p} + O(\theta) \quad , \qquad (7)$$

where $\dot{H}$ is the net radiation source term for the layer (principally nocturnal cooling by IR flux) and C_p is the specific heat at constant pressure for air. The additional effects included are advection, entrainment, and lateral diffusion.

Pollutant Concentration

$$\frac{\partial \overline{\rho s}(\eta - h)}{\partial t} + \frac{\partial}{\partial x_i} \overline{\rho u_i s}(\eta - h) = \dot{m}\, s' + \dot{S} + O(s) \quad , \qquad (8)$$

where s and s′ are the pollutant mixing ratios in the drainage and upper layers and $\dot{S}$ is the source rate term accounting for point or distributed sources of a pollutant. The background mixing ratio is assumed to be constant. In addition, Eq. (8) includes advection and lateral diffusion.

Each of the equations, Eqs. (5)-(8), contains vertically averaged terms to account for the possibility that there may be vertical gradients. A particularly strong gradient of velocity is expected because it must vanish at the surface. At best, the effect of profiles can only be taken into account in an inexact way. We assume that each quantity has a fixed profile as a function of height scaled to the layer thickness; that is,

$$\phi(Z) = \phi_o f_\phi \left(\frac{Z}{\eta - h} \right) \quad ,$$

where $\phi_o = \phi(Z = \eta - h)$ and f_ϕ does not depend on horizontal position or time. We can now write Eqs. (5)-(8) as functions of ϕ_o by including averaging factors:

$$\bar{\phi} \equiv \frac{\int_h^\eta \phi(Z)dZ}{\eta - h} = \phi_o \bar{f}_\phi \quad , \text{ where } \bar{f}_\phi = \int_o^1 f_\phi(\sigma)d\sigma \quad , \tag{9}$$

where σ is a scaled height variable. For example, the mass equation becomes

$$\bar{f}_\rho \frac{\partial\, \rho_o(\eta - h)}{\partial t} + \overline{f_{\rho u}} \frac{\partial}{\partial x_i} \rho_o u_i^o(\eta - h) = \dot{m} \quad ,$$

where $\bar{f}_\rho$ and $\overline{f_{\rho u}}$ are constants determined from Eq. (9) and the asssumed σ-dependence of ρ and u_i. The remaining equations can be derived similarly. The profile coefficients are to be chosen either from data or simple theory; SIGMET calculations[4] of profiles can also be used as a data source. Using the above relationships, we can form the average of any combination of quantities and express it in terms of convenient quantities for numerical evaluation. For example, the momentum flux term can be written

$$\overline{\rho u_i u_j} = (u_i)_o \overline{\rho u_j} \frac{\overline{f_{\rho u^2}}}{\overline{f_{\rho u}}} \quad ,$$

where we assume that the profiles of the two velocity components are the same. In preliminary calculations we have chosen $f_u(\sigma) = \sigma^{1/7}$, which approximately describes a neutral boundary layer. With this representation $\overline{f_u} = 7/8$ and $\overline{f_{u^2}} = 7/9$. More accurate boundary profiles are expected to affect the calculations weakly.

Entrainment is a turbulent mixing process at a shear layer. The drainage layer is defined by an inflection point in the vertical temperature profile (Fig. 2).

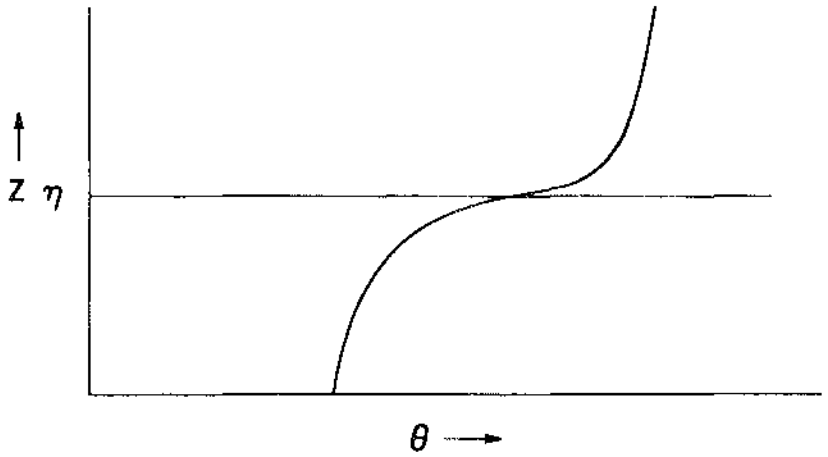

Fig. 2. Description of drainage layer.

The layer also exhibits wind shear across the temperature inflection. The layer becomes thicker as the cold front diffuses into the warmer air of the upper layer by turbulent entrainment. We estimate the rate of diffusion using a constant flux approximation

$$\dot{m} = \bar{\rho} \frac{dx_o}{dt} = \frac{\bar{\rho} D_v}{x_o} \quad , \tag{10}$$

where $x_o = \eta - h$ and D_v is the vertical diffusivity caused by turbulent mixing. Estimating D_v from boundary-layer expressions as a function of relative velocity and $\theta - \theta'$, we calculate $\dot{m}$ for each cell at each cycle for use in Eqs. (5)-(8). The simple entrainment prescription of Eq. (10) deserves to be re-examined in the future. Zeman's analyses[5,6] of stable boundary layers, which take into account field data, laboratory experiments, and second-order closure modeling, may provide an improved formulation.

III. NUMERICAL FORMULATION AND CALCULATIONS

The drainage flow equations, Eqs. (5)-(8), have been programmed as an explicit difference equation system. The equations are evaluated in conservative form on a staggered grid of points. The equations are conditionally stable with the time interval limited by convective, diffusive, and gravity wave inequalities.

The equations are solved sequentially, taking into account all terms of each equation before proceeding to the next equation. Advection in the horizontal directions is calculated using the Crowley second-order method with

doner cell flux limiter. The equations are otherwise second order in space and first order in time. Horizontal diffusion and vertical entrainment are based on empirical boundary-layer turbulent diffusion coefficients, which are a function of wind speed and stability class.

IV. ONE-DIMENSIONAL DRAINAGE FLOW CALCULATIONS

The formulation of Sec. II has been incorporated into the SHALO drainage flow computer code and several calculations have been carried out on the Los Alamos computers. In this section we describe the time-dependent flows in one horizontal dimension; this description verifies the formulation and displays various properties of the flow.

The drainage flow formulation is a generalization of the shallow fluid approximation, which can be recovered as a limiting case. We have taken advantage of this property to verify that previously obtained results can be duplicated with the appropriately modified SHALO code. A careful analytical and numerical investigation of flow over an isolated obstacle was performed by Houghton and Kasahara.[7] They identify several regimes, defined by the Froude number of the initial flow and the height of the obstacle, within which the character of the flow changes. We have duplicated their results by modifying SHALO (1) to eliminate the temperature calculation and (2) to simulate an incompressible atmosphere by selecting the layer thicknesses to be a very small fraction of the atmospheric scale height. The test problems, which include subcritical and supercritical flow over the peak, as well as cases containing hydraulic jumps upstream and downstream of the peak, are contained in the Appendix.

Although the above problems check some of the terms of SHALO and contain interesting flow features, they do not display the characteristics of greatest relevance to drainage flow over complex terrain. To illustrate some of these properties, several additional flow calculations having one horizontal dimension have been carried out. In one set of calculations, which are not illustrated here, drainage layers from adjacent parallel ridges progressively filled the intervening valley. Over the ridges the layer thickness was greatly decreased by the divergent flow, whereas in the valley hydraulic jumps formed to decelerate the down-slope flow.

V. TWO-DIMENSIONAL DRAINAGE FLOW CALCULATIONS

In the more realistic topography of complex terrain regions, we expect that several features of the flow will be exhibited, such as the joining of

flows from several canyons and the pooling of the flow in valleys, in addition to those features of down-slope flow and hydraulic jumps shown by the simpler topography. The Coriolis force is also expected to modify the flow to some extent. Our initial application of SHALO to the geysers area of northern California (Fig. 3) was conducted to gain some insight into the drainage flow physics. We used the results from the September 1980 ASCOT measurements[8] program for this purpose. A test problem was run with a 45 x 28 cell grid (Fig. 3) with each cell 190 m on a side. The dimensions of the entire grid were 8.4 x 5.1 km. The terrain elevation varied from 361 to 1439 m. The simulation started at 6 p.m. (1800) and terminated at midnight (2400). The development of pooling near Anderson Springs (slice 1) and the coalesced flow through the region near Diamond D Ranch (slice 2) are shown in Figs. 4 and 5, respectively. By 2400 hours the pooled layers, showing as three peaks in Fig. 4, are nearly 60 m deep, in general agreement with observation. In Fig. 5, the three peaks have coalesced into an outflow layer peaked at cell 9, as the result of the convergence of three valleys. The layer peak centered near cell 25 in Fig. 5 is due to an unrelated valley.

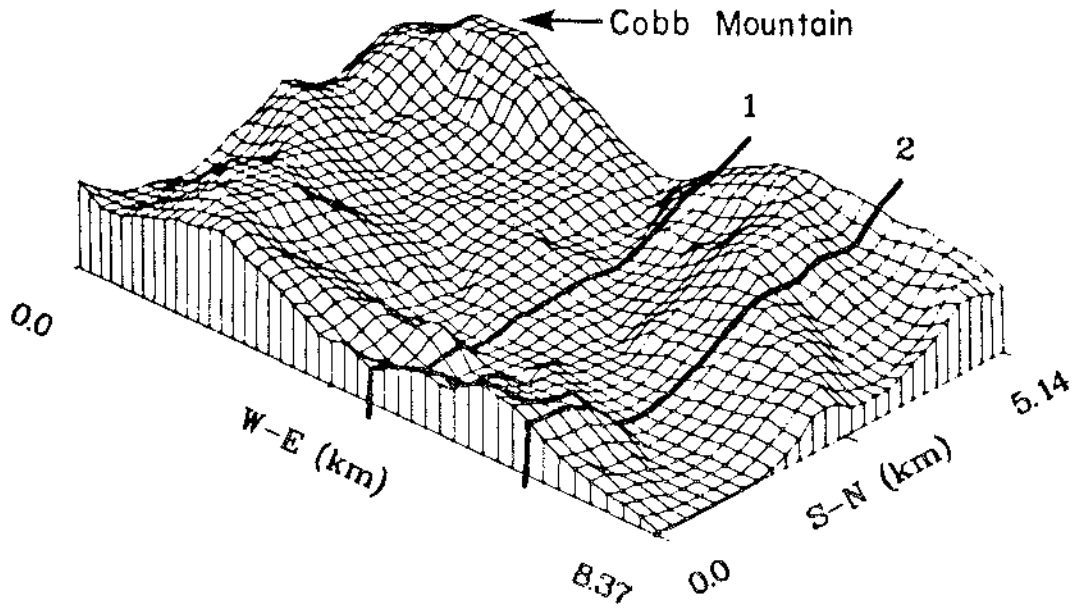

Fig. 3. Geysers area terrain showing slices 1 and 2.

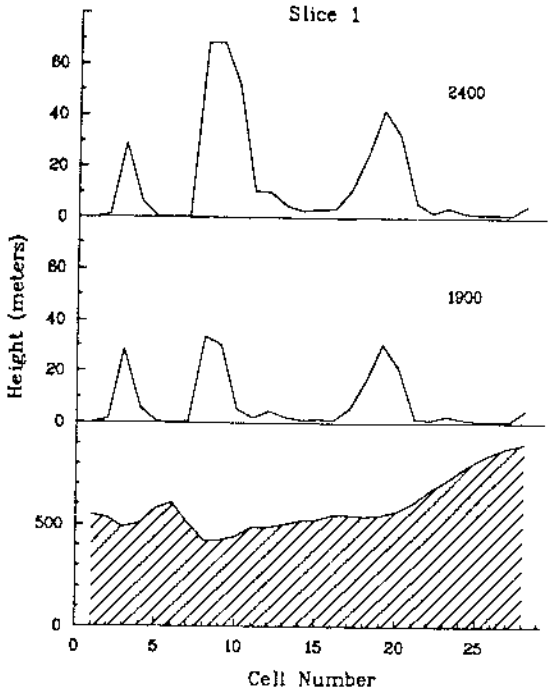

Fig. 4. Depth of drainage flow layer at slice 1 for times 1900 and 2400. The terrain height is also included (bottom curve).

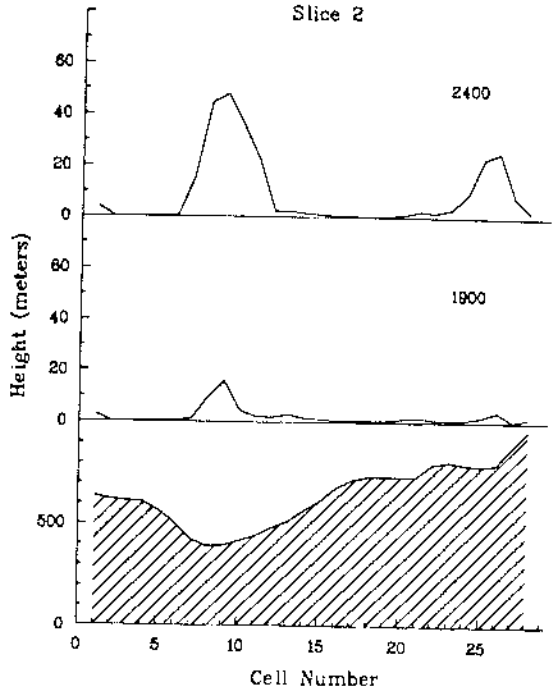

Fig. 5. Depth of drainage flow layer at slice 2 as in Fig. 3.

VI. SUMMARY AND CONCLUSIONS

An approximate formulation of the problem of nocturnal drainage flow has been incorporated into a computer code. This formulation, representing a generalization of the shallow fluid approximation, is applicable to complex terrain and accounts for many of the salient physical effects exhibited by drainage flow. These include the dynamics of the katabatic flow, radiation cooling, surface drag, entrainment of the overlying layer, the Coriolis force, and interaction with the synoptic flow. Sample calculations have been performed in one and two horizontal dimensions. These calculations exhibit a number of interesting qualitative flow features that have been observed, such as thinning of the layer over ridges and pooling in valleys. We also found hydraulic jumps in the flow.

The calculation shows qualitatively correct behavior at modest computational cost. Several processes that are represented parametrically can probably be tuned by comparison with data. Also, by virtue of the low cost of calculations, the model can be applied widely to gain experience in how to best use the output. We suggest that a program of additional comparisons with data, development of improved parameterizations, and employment of more sophisticated graphs is warranted.

Although the model has these advantages, it also is limited by its lack of vertical resolution. The more detailed description afforded by the truly three-dimensional model is necessary for a more complete understanding of this vertical structure. In addition, comparisons with such calculations will indicate the limitations more quantitatively and suggest methods to improve the SHALO drainage flow formulation.

APPENDIX

COMPARISON TO THE ANALYTIC AND NUMERICAL RESULTS OF HOUGHTON AND KASAHARA[7]

Tests of the code SHALO were made against asymptotic mathematical solutions of the shallow fluid equations:

$$\frac{\partial U}{\partial t} + U \frac{\partial U}{\partial X} + g \frac{\partial \phi}{\partial X} + g \frac{\partial H}{\partial X} = 0 \qquad \text{(A-1)}$$

and

$$\frac{\partial \phi}{\partial t} + \frac{\partial}{\partial X} (\phi U) = 0 \qquad \text{(A-2)}$$

for flow over an isolated obstacle (Fig. A-1).

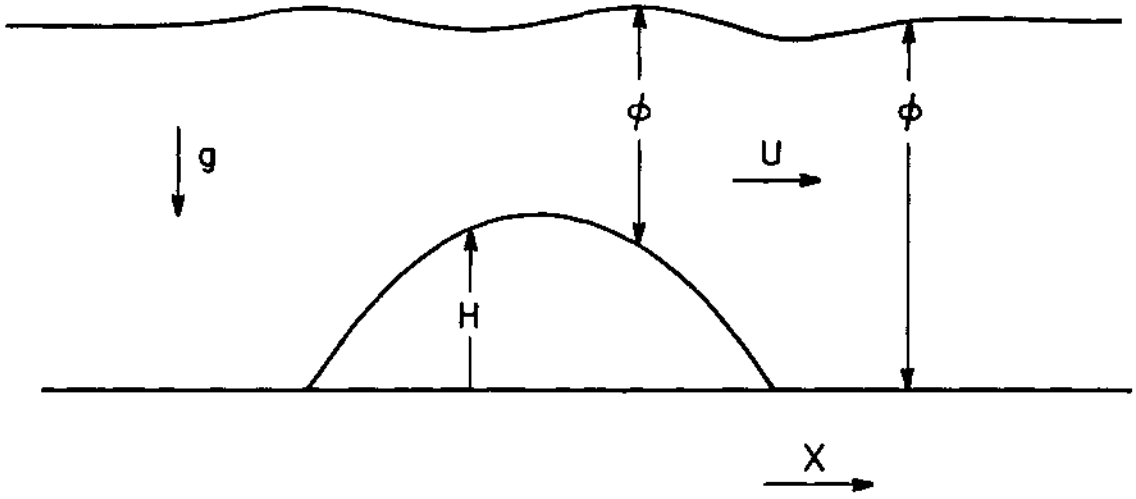

Fig. A-1. Cross section of one-layer model.

$$H(X) = H_c \left(1 - \frac{X^2}{a^2}\right) \text{ for } 0.0 \; |X| \leq a; \qquad H(X) = 0 \text{ for } |X| > a.$$

The results of these mathematical solutions are described in terms of F_o ($= U_o/\sqrt{gh_o}$) and M_c ($= H_c/h_o$), where H_c is the height of the crest and h_o is the height of the approaching fluid.

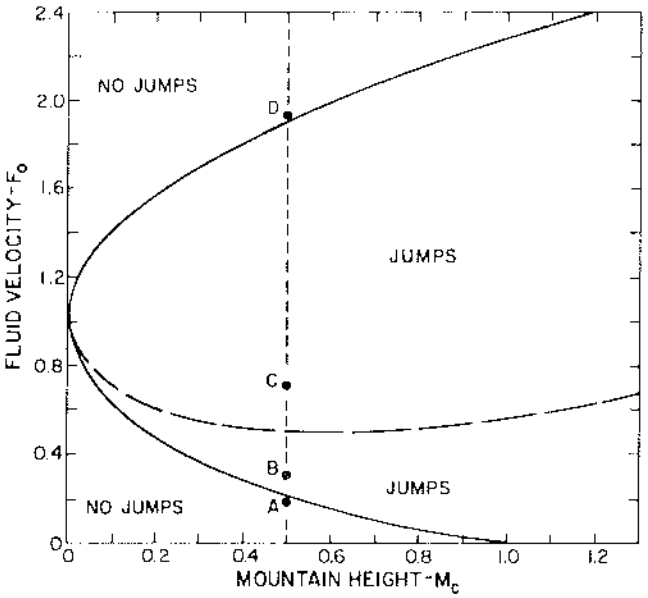

Fig. A-2. Classification asymptotic flow conditions.

The results from the Houghton-Kasahara numerical integration of Eqs. (A-1) and (A-2) for case A are shown in Fig. A-3.

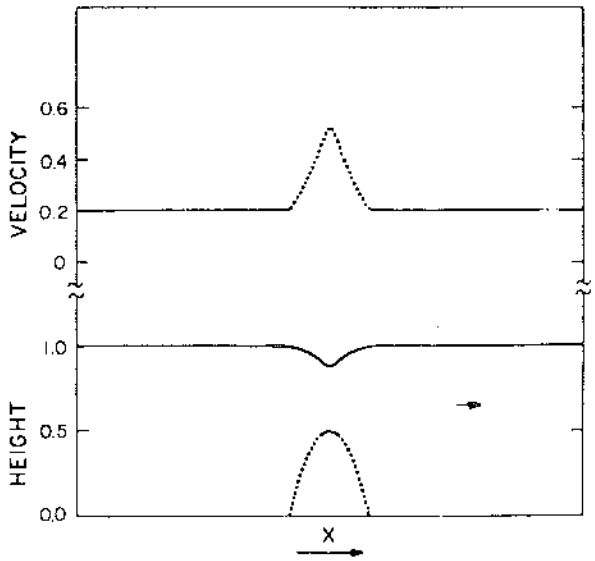

Fig. A-3. Numerical results for case A.

The equivalent results from SHALO are shown in Fig. A-4.

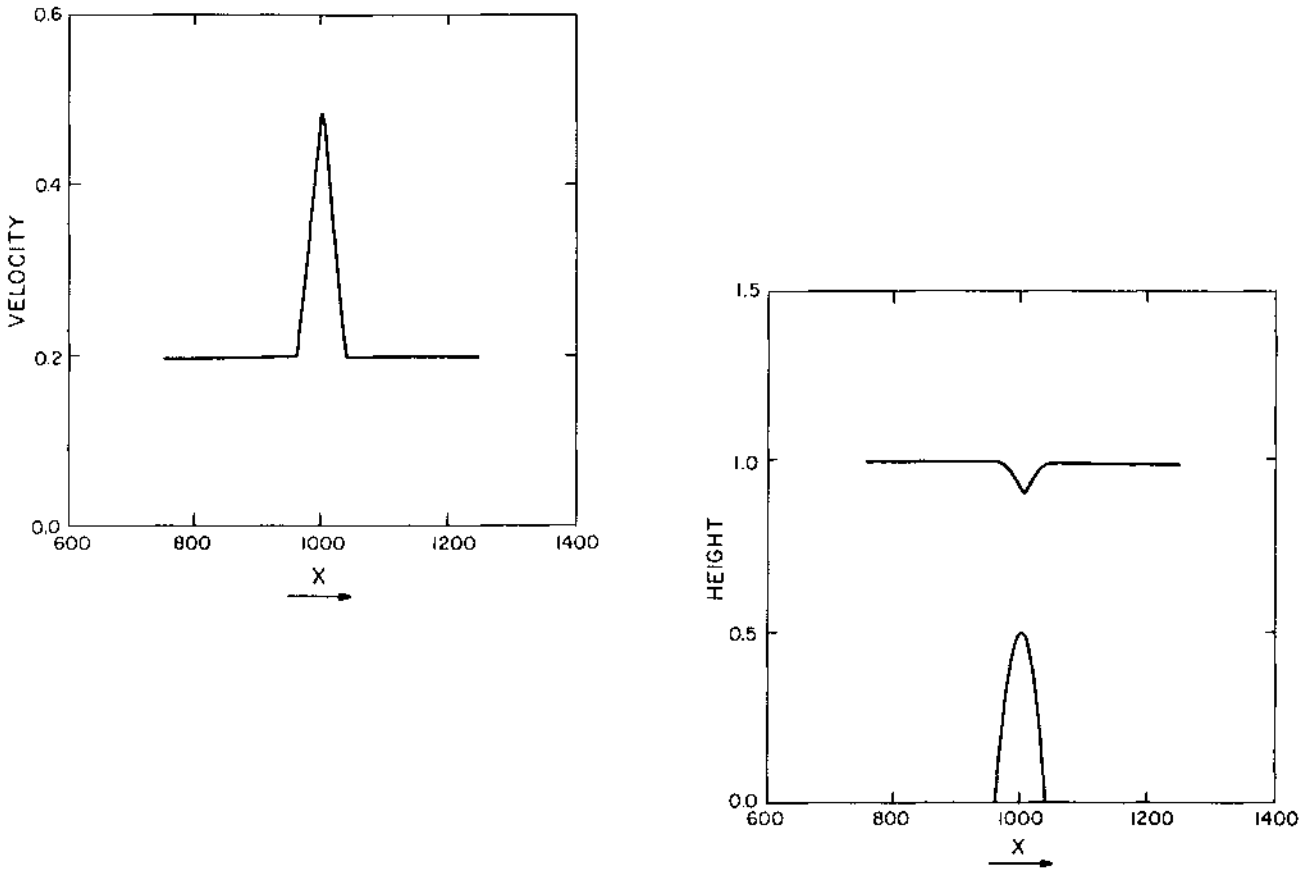

Fig. A-4. SHALO results for case A.

The parameters of these calculations are those of a laboratory experiment by Long[9]: h_o = 20 cm, a = 40 ΔX, and ΔX = 1.0 cm. For case B the Houghton-Kasahara results are shown in Fig. A-5 and the SHALO results in Fig. A-6.

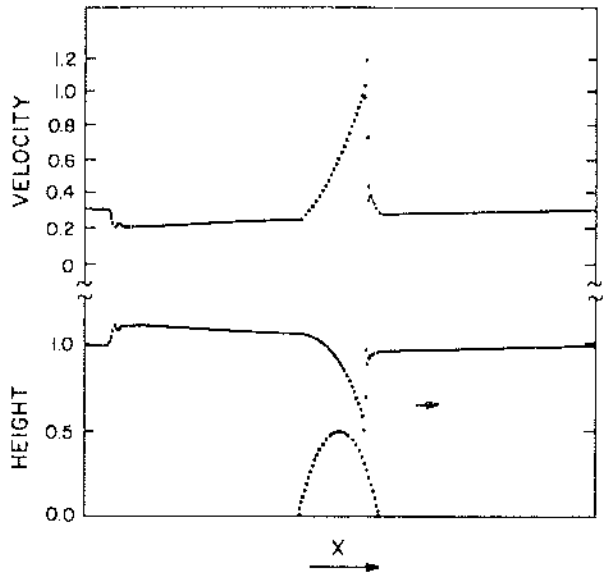

Fig. A-5. Numerical results for case B.

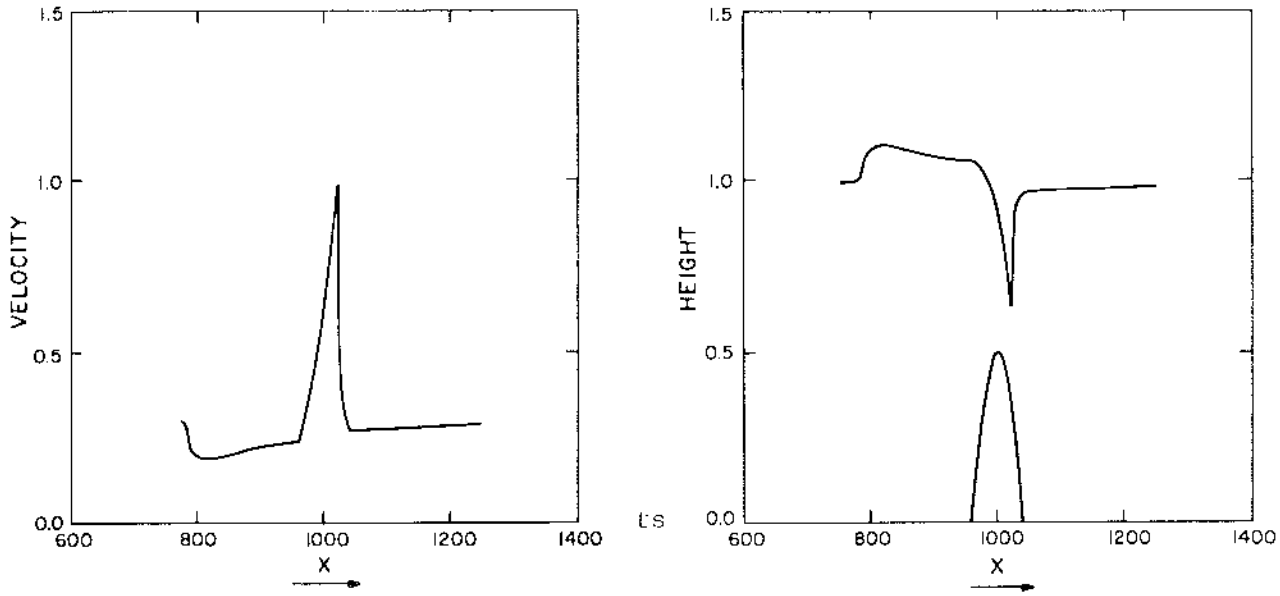

Fig. A-6. SHALO results for case B.

The boundaries at ±L (L = 1000 ΔX) are sufficiently distant from the obstacle to delay reflected waves in the solution. From the stationary lee jump solution (case C), we compare the Houghton-Kasahara solution (Fig. A-7) with our results for the downstream-moving lee jump (Fig. A-8)

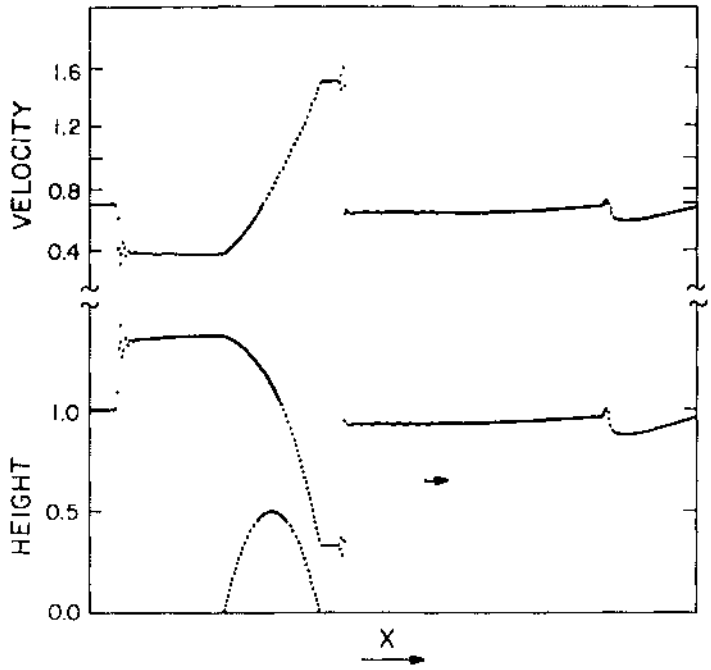

Fig. A-7. Numerical results for case C.

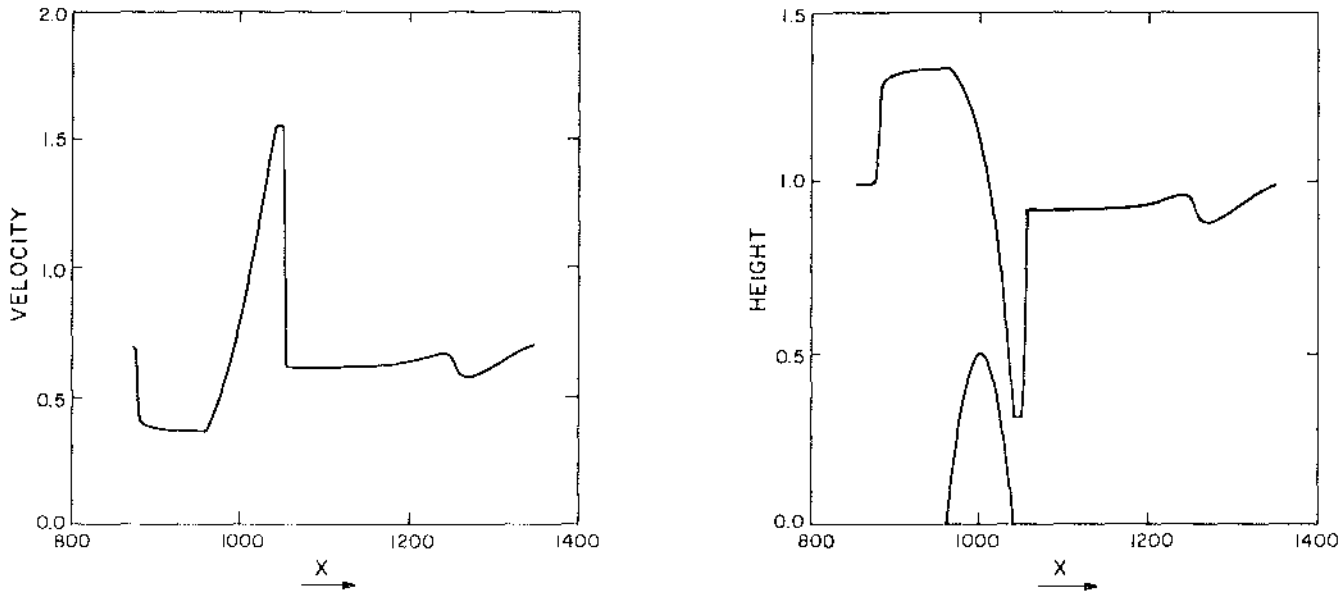

Fig. A-8. SHALO results for case C.

A hydraulic jump of this nature may explain the appearance of rotor clouds in the lee of a mountain: these effects do not occur in linearized theories.

The inferences from these results are that the atmosphere may respond to complex terrain in ways that depend on the Froude number of the complex flow. By simulating the condition of a hydraulic jump for an isolated obstacle, we can expect the code to reveal these conditions properly when the complex terrain interacts with the flow. A single layer will not resolve the boundary-layer flow, but we should obtain a qualitative understanding of the drainage flow in basins or valleys.

The final case studied (case D) has a large Froude number (F_o = 1.9) and does not contain a hydraulic jump. The Houghton-Kasahara solution (Fig. A-9) is compared with the results from SHALO (Fig. A-10).

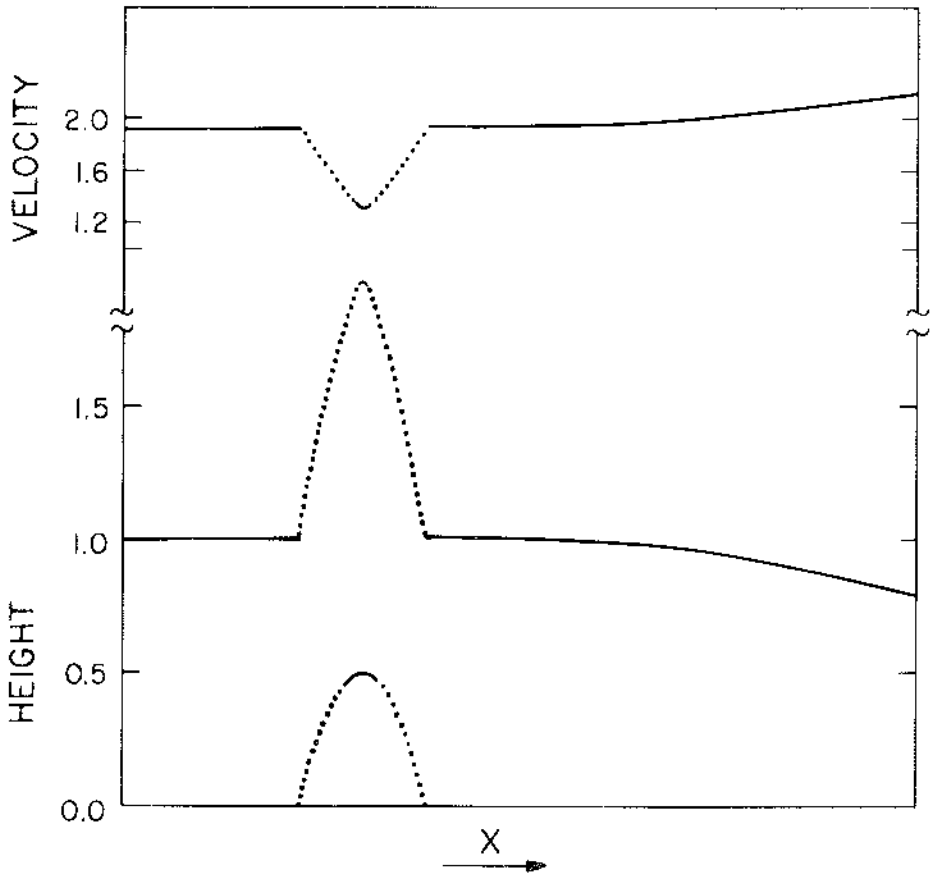

Fig. A-9. Numerical results for case D.

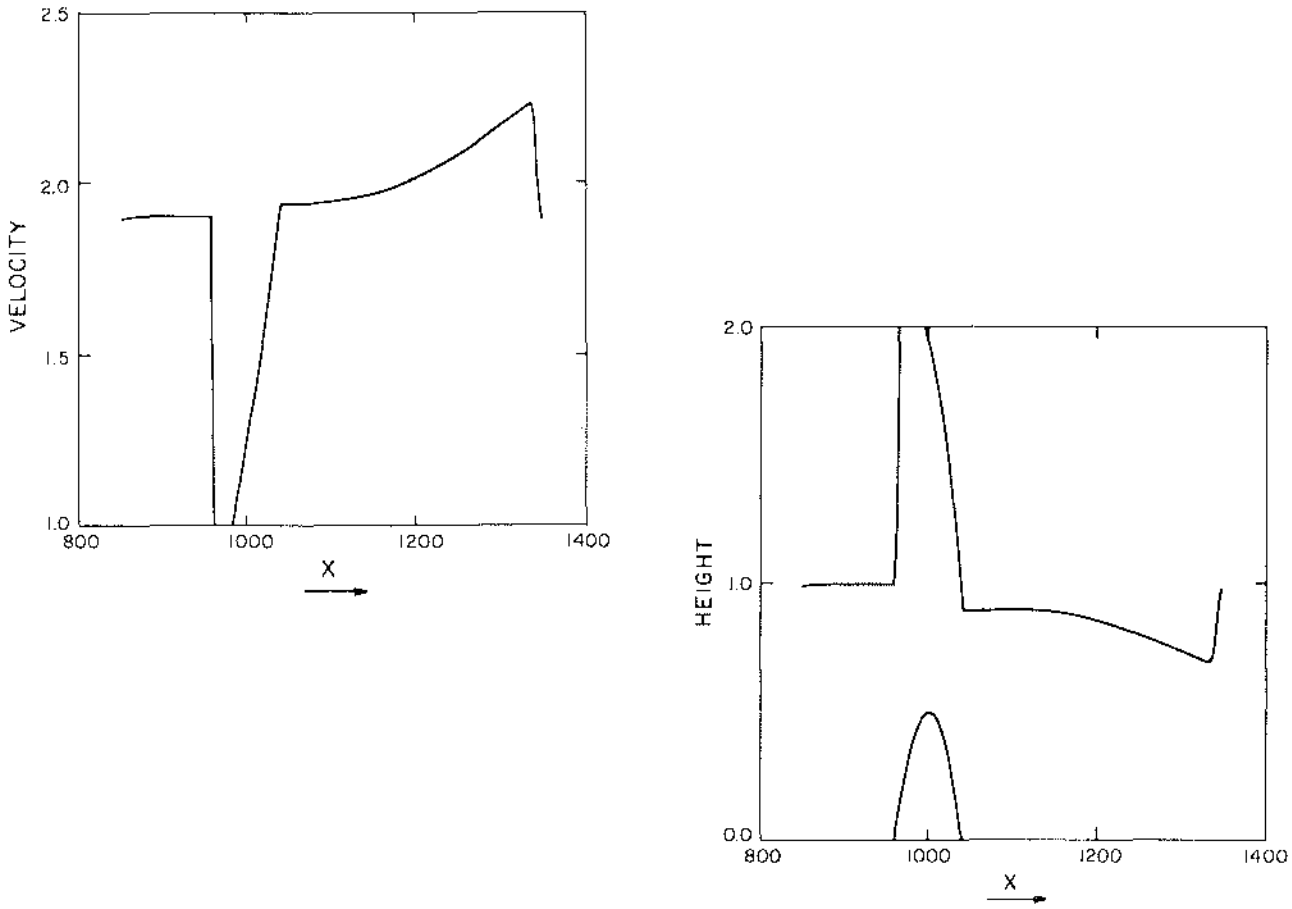

Fig. A-10. SHALO results for case D.

In the supercritical case (D), we were unable to resolve the flow accurately. The effects of a gravity wave in the Houghton-Kasahara calculation are visible on the right side, but the boundary-condition effect appears different in the SHALO results. More work is needed to resolve these differences.

REFERENCES

1. R. L. Lavoie, "A Mesoscale Numerical Model of Lake-Effect Storms," J. Atmos. Sci. 29, 1025-1040 (1972).

2. J. R. Bjorklund and A. G. Tingle, "Study and Investigation of Computer Algorithms for the Solution of the Shallow-Fluid Equations as a Means of Computing Terrain Influences on Wind Fields," H. E. Cramer, Inc., technical report 73-302-01 (1973).

3. W. Ohmstede, "The Dynamics of Material Layers," Atmospheric Sciences Laboratory report ASL-TR-0036 (1979).

4. C. G. Davis and B. E. Freeman, "Modeling Drainage Flow with SIGMET," US/DOE ASCOT report 81-1 (1981).

5. O. Zeman, "Parameterization of the Dynamics of Stable Boundary Layers and Nocturnal Jets," J. Atmos. Sci. 36, 792-804 (1979).

6. O. Zeman, "The Dynamics and Modeling of Heavier-Than-Air Cold Gas Releases," Lawrence Livermore Laboratory report UCRL-15224 (1980).

7. D. D. Houghton and A. Kasahara, "Nonlinear Shallow Fluid Flow Over An Isolated Ridge," Comm. Pure Appl. Math. 21, 1-23 (1968).

8. P. H. Gudiksen, "ASCOT Data From The 1979 Field-Measurement Program in Anderson Creek Valley, California," US/DOE ASCOT report 80-9 (1980).

9. R. R. Long, "Some Aspects of the Flow of Stratified Fluids II, Experiments with a Two-Fluid System," Tellus 6, 97-115 (1954).

Printed in the United States of America
Available from
National Technical Information Service
US Department of Commerce
5285 Port Royal Road
Springfield, VA 22161

Microfiche (A01)

Page Range	NTIS Price Code
001-025	A02
026-050	A03
051-075	A04
076-100	A05
101-125	A06
126-150	A07
151-175	A08
176-200	A09
201-225	A10
226-250	A11
251-275	A12
276-300	A13
301-325	A14
326-350	A15
351-375	A16
376-400	A17
401-425	A18
426-450	A19
451-475	A20
476-500	A21
501-525	A22
526-550	A23
551-575	A24
576-600	A25
601-up*	A99

*Contact NTIS for a price quote.

UNITED STATES DEPARTMENT OF ENERGY
P.O. BOX 62
OAK RIDGE, TENNESSEE 37830

OFFICIAL BUSINESS
PENALTY FOR PRIVATE USE. $300

POSTAGE AND FEES PAID
UNITED STATES
DEPARTMENT OF ENERGY

U S MAIL

FS- 1
UNIVERSITY OF UTAH RESEARCH INSTITUTE
ATTN PHILLIP M WRIGHT
EARTH SCIENCE LAB
420 CHIPETA WAY, SUITE 120
SALT LAKE CITY, UT 84108